Science of the Total Environment 719 (2020) 134984

Contents lists available at ScienceDirect

Science of the Total Environment

journal homepage: www.elsevier.com/locate/scitotenv

Impact of port emissions on EU-regulated and non-regulated air quality indicators: The case of Civitavecchia (Italy)

Gian Paolo Gobbi *, Luca Di Liberto, Francesca Barnaba

Institute of Atmospheric Sciences and Climate, ISAC-CNR, Via Fosso del Cavaliere, 100, 00133 Rome, Italy

HIGHLIGHTS

- Meteorology, ship positioning and engine type influence the port role on nearby city air quality.
- The port activities contribute 33% of NO_2 43% of PM_{10} and 60% of SO_2 causing no exceedance of the AQ limits
- Low Sulphur fuels do not prevent release of pollutants as ultra-fine particles, and black carbon.
- High loads of black carbon and ultrafine particles coexist with admitted loads of NO_2, SO_2, and PM.

GRAPHICAL ABSTRACT

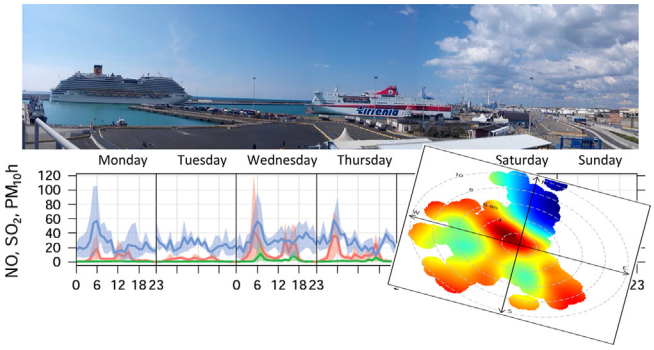

ARTICLE INFO

Article history:
Received 8 July 2019
Received in revised form 23 September 2019
Accepted 13 October 2019
Available online 2 November 2019

Editor: Pavlos Kassomenos

Keywords:
Port emissions
Port-city pollution
Marine fuels
Ultra-fine particles
Black carbon

ABSTRACT

Current shipping activities employ about 3% of the world-delivered energy. Most of this energy is conveyed by diesel engines. In Europe, release of NO_x and particulate matter (PM) from shipping is expected to equal the road-transport one by the year 2020. This paper addresses a typical central Mediterranean city-port condition to evaluate the relative contribution of shipping activities to the local air quality. A 3-year long air quality dataset collected at the boundary between the port of Civitavecchia (the major port in central Italy) and the city itself was analyzed to evaluate the long-term, relative contribution of the port and of the city at determining the loads of EU-regulated pollutants (NO_2, PM_{10} and SO_2). In addition, black carbon and ultrafine-to-coarse particles data collected along a short-term, intensive campaign were used to assess the port's role at emitting these unregulated pollutants. Cross-analysis of the measurements, allowed to assess which shipping-related activities and port's sectors represent the principal emitters. At the city-port boundary, the annual share of regulated pollutants originating in the port area by shipping and ground movements is of 33% for PM_{10}, 43% for NO_2, and 60% for SO_2. Analysis of non-regulated pollutants shows the in-port, high polluting potential of some ship categories, in particular those employing low-sulfur but poorly refined oils. These conditions appear to be more often associated with Ro-Ro passenger ships. Piers closest to the Civitavecchia urban settlements are also observed to host the largest emissions. Meteorology and location of the piers with respect to residential areas are confirmed to govern the port's share at impacting the city air quality. Even though air quality thresholds for regulated pollutants are not exceeded in Civitavecchia, constant consideration of an enlarged set of environmental variables should drive actions implemented to mitigate the port's impact onto the nearby city's air quality.

* Corresponding author.
E-mail address: g.gobbi@isac.cnr.it (G.P. Gobbi).

https://doi.org/10.1016/j.scitotenv.2019.134984
0048-9697/

1. Introduction

The globalization of industrial and agricultural processes makes maritime transport (shipping) a fundamental sector of the world economy (UNCTAD, 2017; EEA, 2017a). Currently, over 80% of the world trade is carried by sea (e.g., Cullinane, 2014; UNCTAD, 2017). Overall, 25% of world delivered energy consumption is employed for transport. About 75% of this energy is employed for road transport, 12% for shipping and 12% for air transport (EIA, 2016).

The majority (95%) of the world's shipping fleet runs on diesel engines (Deniz et al., 2010), and it is expected that shipping energy use and emissions will keep growing in the near future (Buhaug et al., 2009; Eyring et al., 2010; UNCTAD, 2017).

International shipping generates between 1.6% and 4.1% of global CO_2 emissions (Psaraftis and Kontovas, 2009), a minor contribution with respect to road emissions (21% of global CO_2 emissions) or energy production (35%) (Buhaug et al., 2009). Still, about 15% of global anthropogenic NO_x, and 5–8% of SO_x emissions are attributable to ocean-going ships (Eyring et al., 2005; Corbett et al., 2007, Maragkogianni et al., 2016).

Since 1990, the European Union (EU) transport-related emissions of air-quality-impacting species have been reducing with the exclusion of the international aviation and shipping sectors, whose particulate matter (PM), NO_x and SO_2 releases have increased instead (EEA, 2017b). In 2015, the transport sector (including road, aviation and shipping) contributed <20% of the total EU emissions of $PM_{2.5}$, PM_{10}, and SO_2, while emitting 55% of total NO_x. Shipping generated over 90% of transport-related SO_2 emissions, while its $PM_{2.5}$, PM_{10}, and NO_x emissions represented 45, 28, and 35%, respectively (EEA 2017b). In Europe, despite a four-time lower use of energy (EEA, 2017c), shipping releases of NO_x and PM are expected to equal road-transport ones in 2020, (EEA, 2013, Aksoyoglu et al., 2016). Such large NO_x, SO_2 and PM emissions originating from marine transport are caused by the predominant use of scarcely regulated diesel engines, which, on turn, run on low-grade oil (e.g., Cullinane, 2014).

Common oils used in marine engines are rich in sulfur and residuals as the heavy fuel oil (HFO, with sulfur content S > 1.5%). Conversely, the more expensive low-sulfur, partly-refined marine diesel oil (MDO, $S \leq 1.5\%$), and marine Gas Oil (MGO, $S \leq 0.1\%$) are only employed to respond to specific constraints (e.g., Buhaug et al., 2009). For instance, low sulfur, unrefined oil is often employed in sulfur emission control areas (SECAs.). Still, this limitation in sulfur content does not prevent the emission of other major pollutants as NO_x, ash, heavy metals, and organics. Currently, the sulfur content of oil to be used in EU ports and emission control areas (ECA) is of 0.1%, while it is of 1.5% in non-ECA, EU waters (EU Directive 2005/33/CE), and of 3.5% in all other conditions. Starting 2020, global limits will converge to 0.1% fuels in ECA and port environments and to 0.5% in all other conditions (Buhaug et al., 2009; EEA, 2013). As a reference, EU road diesel has a maximum sulfur content of 0.001%. Reducing from 0.5% to 0.1% the oil's sulfur content results into a cut of about 50% in PM emissions (Buhaug et al., 2009). Reducing sulfur content of marine fuels can reduce PM mass, not necessarily soot, ashes and related health effects (e.g., Oeder et al., 2015). In this respect, aftertreatment of diesel exhausts as done by emission gases conditioning systems (EGCS) represents the mandatory step to abate such emissions (e.g., EEA, 2013; Barregård et al., 2014; Winebrake et al., 2009).

Diesel engines are strong emitters of both primary and secondary PM (e.g., Winnes and Fridell, 2009; Lack, and Corbett, 2012). Diesels primary PM, mostly emitted as ultra-fine particles (i.e., smaller than 100 nm in diameter), includes soot, ash and a variety of organics as polycyclic aromatic hydrocarbons (PAHs), with strong light absorption properties (e.g., Buhaug et al.,2009, Lack and Corbett, 2012). These dark PM emissions are commonly addressed as black and brown-carbon (BC and brC), respectively, e.g., Andreae and Gelencsér (2006). Shipping secondary PM emissions include sulfates, nitrates and organics (e.g, Viana et al., 2014; Anderson et al., 2015). In terms of mass, shipping contributes more PM in the form of secondary particles with respect to primary ones (Viana et al., 2014).

Diesel emissions as a whole have been defined as "carcinogenic through genotoxicity" by the International Association of Cancer Research (IARC, Benbrahim-Tallaa et al., 2012). BC, an important component of diesel PM emissions, is also reported as a robust indicator (more than PM_{10} or $PM_{2.5}$ metrics) of PM-induced mortality and morbidity (WHO, 2012). In a similar way, NO_2, another significant emission of ship diesels, is known to bear adverse health consequences for humans (e.g., WHO, 2013).

In 2007, global mortality caused by ship emissions was estimated at 60,000 per year, with an expected growth of 40% by 2012 (Corbett et al. (2007)). In fact, Sofiev et al. (2018) estimate the 2020 global mortality due to shipping emissions will grow to about 250,000.

The Mediterranean Sea embodies only 0.7% of the world ocean's surface. Still, 5% of the global shipping transits over this sea (UNCTAD, 2012; Eyring et al., 2010). The Mediterranean region, and the Italian coast in particular, are one of the world hotspots in terms of shipping pollution and consequent health effects (Winebrake et al., 2009, Sofiev et al., 2018). In this respect, emissions from ship traffic are expected to have a significant, increasing impact on inland air quality (Viana et al., 2014, Aksoyoglu et al., 2016). Overall, between 10 and 30% of $PM_{2.5}$ in large Mediterranean coastal cities originates from shipping (Thunis et al., 2018).

Due to maneuvering, fueling and hoteling phases, ship-generated air pollution can be rather large in port areas (e.g., Barregård, et al., 2014, Murena et al., 2018). Involving non-optimal engine loads, maneuvering can generate much more pollution (3–6 times) than cruising and hoteling phases (Petzold et al., 2010; Moldanova et al., 2013; Lack and Corbett, 2012). When at berth, most ships supply their services by means of auxiliary diesel engines. Depending on ship type, the energy needed during hoteling ranges between 30% and 50% of the one employed at cruising (e.g., Tzannatos, 2010). Overall, in-port emissions of NO_x and SO_2 represent 5–6% of the total generated by ships in all their navigation phases (Whall et al., 2002).

All these elements point out that in both port areas and port cities important fractions of air pollutants can originate from ships (Tzannatos, 2010; Cullinane, 2014; Viana et al., 2014). To evaluate and reduce risks associated with atmospheric pollution, it is therefore important to know both amount and type of pollutants attributable to shipping, particularly in port-cities. This paper addresses previously unobserved aspects of air pollution in the Mediterranean port city of Civitavecchia, the major passenger-commercial port serving the Rome area, in central Italy. In fact, EU air quality thresholds for PM_{10}, SO_2, and NO_2 (as well as for all the regulated pollutants) are rarely exceeded in Civitavecchia (Section 3.1.2). Still, epidemiological studies show higher mortality of residents in this city (mainly related to respiratory and cancer pathologies) with respect to the surrounding region (Fano et al., 2004, Fano et al., 2006). Recently, a new epidemiological study confirmed a 31% increase in mortality due to lung cancer and a 51% increase due to neurological diseases for people residing within 500 m from the port area (Bauleo et al., 2018). As a consequence of these ongoing health issues, Civitavecchia become one of the most monitored sites in central Italy.

This study provides original insights about the role of the port at influencing the air quality in Civitavecchia. This is done by analyzing measurements of both regulated (NO_2, PM_{10} and SO_2) and

unregulated atmospheric pollutants (black carbon, and particle size-resolved distributions from the ultrafine to the coarse modes). Principal emitters of these pollutants are inferred through a statistical/graphical analysis coupling observations with wind data to determine their azimuthal provenance and relevant loads. This approach allows to interpret large, multi-variate data-sets without need for modeling or analytical assumptions. Based on this analysis, we separate the port's (shipping plus ground activities) from the city contributions to the Civitavecchia air quality indicators. Recommendations about improvements to mitigate the port's impact on the city regulated and "unregulated" air quality are formulated.

2. Methods

2.1. The study area

The port of Civitavecchia (42.1°N, 11.8°E) is located on a flat, hill-edging headland of the Tyrrenian coast of central Italy (Fig. 1a). It extends to the NW of the city for about 3 km (Fig. 1b and 1c). In addition to regular ferry links (Ro-Ro passenger) to Sardinia, north Africa, and Spain, the port hosts an important traffic of cruise ships, cargo ferries, and carrier ships summing-up to some 3000 ship movements per year (about 1500 Ro-Ro passengers, 1000 cruise, 500 cargo/carriers), involving 4 million passengers, 1 million vehicles, and some 16 Mt of goods (Rome Ports Authority, 2014 data). Twenty-six port piers serve mainly Ro-Ro passengers ships in the southern port area, cruise ships in the central-west area, and cargo and goods-carriers in the central-north areas (Fig. 1c). The whole port area is flat, with sparse buildings spanning maximum heights of 10–15 m (Fig. 1b). Port extension works are underway in the NW sector, i.e., north of the cargo area (Fig. 1c). Road transport in the port sums up to about 1.000.000 visiting-vehicles per year. Just inland of the central-northern portion of the port, jet-fuel, gasoline, diesel, and heavy-fuel tanks store oil products unloaded by tankers (about 1Mt/year) through an offshore pipeline located some 2 km off the coast.

Some 1.5 km NW of the northern, heavy-duty vehicles port's entrance (Varco Molinari), stands the ENEL generating board, 1980 MW, coal-fired power plant of Torrevaldaliga Nord (TVN, yellow ellipse in Fig. 1c). Here ships unload coal to dome-covered deposits directly at the plant's pier, detached from the port's area. Emissions from this power plant are released out of a 250 m high chimney, at a maximum emission allowance of 2100 tons of SO_2, 3450 tons of NO_x, 160 tons of PM, 2000 tons of CO, and 195 tons of NH_3 per year (ENEL, 2016). Some 400 m SE of TVN, a second power plant (1200 MW, gas-fired) named Torrevaldaliga Sud (TVS) is operated by Tirreno Power. TVS emissions are released at 90 m MSL, with maximum allowances of 2500 tons of NO_x, and 1500 tons of CO per year. TVN and TVS stand at a distance of 4.5 km from the southern portion of the port, where the entrance named "Varco Vespucci" directly connects to the NW sector of Civitavecchia. Here also stands the air quality station "Arpa Porto" (Fig. 1c, d). The city itself (about 52,000 inhabitants) further extends some 2 km SE along the coast, and some 2 km inland (NE) from this point. The city center is located about 0.7 km SE of the "Varco Vespucci" port entrance (see also Fig. 6).

2.2. Measurements

Our analysis employs "receptor type" observations performed at fixed monitoring stations operated in the port area. The investigation takes into account the main emission sources related to the Civitavecchia port and city activities. Timing of measurements and relevant analyses is given in UTC. Civitavecchia local time is UTC + 1.

2.2.1. Regulated pollutants

Measurements of EU-regulated air pollutants employed in this study, namely NO_2, SO_2, and PM_{10}, were collected by the regional environmental protection agency (ARPA Lazio) at the Arpa Porto station, during the 3-year period May 2013-April 2016. This monitoring station stands exactly at the boundary between the port and the city (Fig. 1c, d), i.e., it is assumed to intercept the most of the air pollution originated in the port area and directed to the city. The type of instrumentation performing the air quality and

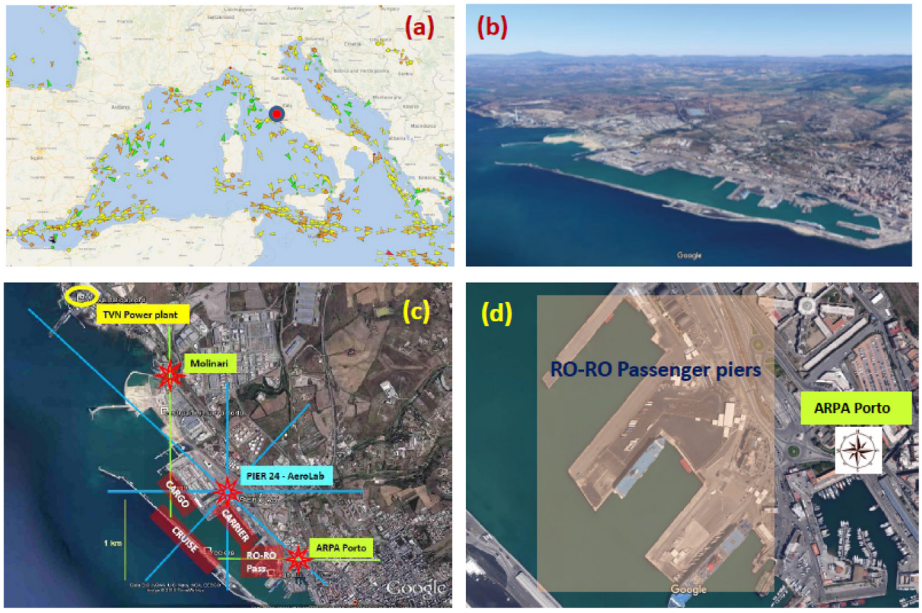

Fig. 1. (a) Location of the Civitavecchia port (red dot), and main shipping routes (ship symbols) in the Mediterranean Sea; (b) aerial view of the port and of the city of Civitavecchia (at the bottom-right corner); (c) mooring piers by ship category, and other significant sites addressed in the paper; (d) location of the Arpa Porto AQ station and Ro-Ro passenger piers. (For interpretation of the references to color in this figure legend, the reader is referred to the web version of this article.)

Table 1
List of the instrumentation/measurements employed in the analysis. Abbreviations indicate, respectively: PM_{10} = particulate matter smaller than 10 μm in aerodynamic diameter; NO, NO_2 = Nitrogen oxide, and dioxide; SO_2 = Sulfur dioxide; AWS = automatic weather station; p = atmospheric pressure; T = temperature; RH = relative humidity, ws, and wd = wind speed, and direction; APS = aerodynamic particle sizer; SMPS = scanning mobility particle sizer; Scattering-Coeff = scattering coefficient; eBC = equivalent black carbon.

Site	Instrument	Measured Variable	Time resol.	Begin date	End date	Data points #
Arpa Porto	Environment MP101M	PM_{10}	1-h	1–4-2013	31–3-2016	24,034
Arpa Porto	Teledyne T200A API	NO + NO_2	1-h	1–4-2013	31–3-2016	23,308
Arpa Porto	Teledyne T100A API	SO_2	1-h	1–4-2013	31–3-2016	22,646
Arpa Porto	Vaisala AWS	p,T,RH, ws, wd	1-h	1–4-2013	31–3-2016	24,690
Pier 24	TSI APS	Size Distribution 0.5–30 μm	5′	05–4-2016	26–4-2016	6274
Pier 24	Tropos SMPS	Size Distribution 0.008–0.7 μm	5′	05–4-2016	26–4-2016	5996
Pier 24	Magee AE33 Aethalometer	eBC	1′	05–4-2016	26–4-2016	31,986
Pier 24	Ecotech Aurora 3000 Nephelometer	Scattering Coeff.	1′	05–4-2016	26–4-2016	31,127
Pier 24	Lufft AWS 700	p,T,RH, ws, wd	1′	05–4-2016	26–4-2016	31,375
Pier 24	Lufft CHM15k	Backscatter profiles 1064 nm	5′	05–4-2016	26–4-2016	6243

meteorological measurements employed in this analysis is listed in Table 1. All variables addressed were measured at 1-h time resolution. All the instrumentation run at Arpa Porto matches the quality assurance and quality control (QA/QC) specifications given in the EC Directive 2008/50/CE (ISPRA, 2014).

2.2.2. Non-regulated pollutants

As a complementary information, high time-resolution measurements of equivalent black carbon (eBC), ultra-fine particles (UFP), and particle size distributions (PSD) have been collected at Pier 24 (Fig. 1c, 42.104 N − 11.778 E, 7 m MSL) by our mobile laboratory AEROLAB, during the month of April 2016. These three metrics are recognized to bear an association with health impairment stronger than PM_{10} (e.g., Benbrahim-Tallaa et al., 2012, WHO, 2013). Pier 24 is located at the core of the port, about 1 km NW of the port Ro-Ro passenger piers and 1.2 km NW of the Arpa Porto station (Fig. 1c). The city center stands about 1 km SE of the Ro-Ro passenger piers. Meteorological variables, and atmospheric backscatter profiles collected by an automated lidar ceilometer (ALC) were also measured at Pier 24 during this campaign. The list of the AEROLAB measurements employed in this analysis is also given in Table 1.

All the in-situ aerosol instrumentation run within the AEROLAB at Pier 24 matches the standard operating procedures and measurement guidelines for aerosol particle variables defined by the ACTRIS (the EU Research Infrastructure for the observation of Aerosol, Clouds and Trace Gases, www.actris.eu), and by WMO/GAW (2016). All these instruments were calibrated within the 4 months preceding the campaign.

2.3. Estimated emissions in the Civitavecchia area

An evaluation of the main pollutants emitted in the Civitavecchia area has been performed to provide an "order of magnitude" reference in support to our analysis. The estimates include emissions from: (i) ships, (ii) city road transport and heating; (iii) TVN and TVS power plants. No quantitative use of these emission estimates is made throughout the paper.

Timing and category of ships calling at the port of Civitavecchia in the period May 2013 - April 2016, as provided by the Rome Ports Authority have been employed to estimate relevant emissions. Table 2 reports the number of ship calls occurred at Civitavecchia in that period. Ships are divided into the four main types calling at this port: (1) Ro-Ro passenger, (2) cruise, (3) bulk material carrier, and (4) cargo. The identification number of relevant mooring piers is also specified in Table 2. Quantity of ships at anchor or moored at the TVN power plant's dock, both stationing being outside the port (Fig. 1c), are reported in the last column. Over this time-span, the port borne some 2700 ship movements per year, 51% made by Ro-Ro-passenger type, 33% by cruise ships, and 8% made by both cargo and bulk carriers. Maximum ship movements occurred in summer and minimized in winter, with a summer to winter decrease of 45% in the case of Ro-Ro Passenger and of 70% for Cruise ships. These data also show the docks closer to the city (the Ro-Ro passenger ones in Fig. 1c, d) to host the largest amount of annual ship traffic.

In accordance with Whall et al. (2002), and EEA (2016), emissions of NO_x, SO_2 and PM originated from ships maneuvering and hoteling in the port have been estimated by considering single ship type and engine power, as provided by the Port Authority records. Engines have been assumed to be medium speed diesels employing marine gas oil (MGO) in all port maneuvering and hoteling phases. Evaluation of the yearly average emissions per ship type are summarized in Table 3. Seasonal estimates of the specific emission daily rates can be derived by combining the data reported in Tables 2 and 3.

Yearly-average emissions attributable to the city's road transport, heating, and to the TVN and TVS power plants are summarized in Table 4. The city emissions have been estimated on the basis of the emission inventories published by the National environmental agency, ISPRA. Emissions generated by road transport have been extracted from the provincial disaggregation of the national inventory (ISPRA, 2010). Conversely, emissions generated

Table 2
Yearly and seasonal average number of calls at the port of Civitavecchia per ship type and mooring pier in the 3-year period 2013–2016 (grand total 9207 calls). Usual mooring pier numbers are reported under the ship type. Ship calls at the TVN power plant pier, or at anchorage outside the port are reported in the last column.

Average period	Ro-Ro passenger 2–14-16–18-20–21	Cruise 10–11-12–13-25S	Bulk carriers 22–23-24	Cargo 25 N-26–27-28	Port Total	Anchor & TVN
Winter	267	86	45	41	439	100
Spring	319	215	57	51	643	102
Summer	480	292	66	55	893	91
Fall	320	289	56	54	719	82
Year	**1386**	**883**	**224**	**202**	**2694**	**375**

Table 3
Estimated yearly emissions (2013–2016 average) per ship category and hoteling pier at the port of Civitavecchia. Estimates of emissions originating outside the port area (off-port anchor and TVN piers) are included in the last row.

Ship type	NO_x [t/year]	TSP [t/year]	SO_2 [t/year]	Piers
Ro-Ro Pax	407.9	13.8	42.3	2–14-16–18-20–21
Cruise	393.9	13.4	40.9	10–11-12–13-25S
Bulk	48.0	1.6	5.0	22–23-24
Cargo	85.7	2.9	8.9	25 N-26–27-28
Port Total	**939.6**	**31.9**	**97.5**	**All Piers**
Port + Anchor + TVN pier	1177.7	40.0	122.2	All piers + Anchor & TVN pier

Table 4
Estimates of annual emissions generated by the TVN and TVS power plants, by road transport, and by heating (November 15-March 15) in Civitavecchia.

Emitter	NO_x [t/y]	TSP [t/y]	SO_2 [t/y]	Reference
TVN	2994	62	1943	ENEL (2016)
TVS	2500	n.a.	n.a.	Ministry of Environment web site
Road	330	22	0	ISPRA (2010, 2018)
Heating	87	112	10	ISPRA (2009, 2018)

by heating (November 15 to March 15) in the city of Civitavecchia have been estimated on the basis of the provincial disaggregation of the national inventory ISPRA (2009), and of the 1990–2016 emissions national inventory (ISPRA, 2018). The TVN power plant emissions have been extracted from the ENEL generating board publication ENEL, 2016. Emissions of the TVS power station have been obtained from the Ministry of Environment web site (https://va.minambiente.it/it-IT/Oggetti/Documentazione/1908/3302).

According to these estimates, release of NO_x from the two power stations is about 5-times higher than the shipping one, and 15-times higher than the city road transport one. Conversely, PM emission from TVN is 6-times the shipping one and 12-times the city road traffic one. In terms of SO_2, TVN emission is 17-times the shipping one. Emissions from the TVN and TVS plants are released at a single point, positioned respectively at 250 m and 90 m MSL, some 4.5 km away from the city, while port emissions occur between ground and some 60 m MSL, along a 2 km-long strip, partly encompassed in the urban area (Fig. 1).

Comparison of emission estimates from shipping ("port total" in Table 3) and the city ("road" plus "heating" in Table 4) indicates shipping releases to be larger in terms of NO_x (by a factor $\approx$ 2-3), PM_{10} (by a factor $\approx$ 2 in non-heating seasons), and SO_2 (by a factor $\approx$ 10). Conversely, PM emissions from the city are expected to dominate during the heating season. In the annual average, city emissions of PM are a factor $\approx$ 3 larger than the port's ones. The analysis presented in the next sections (Section 3.1) will provide an observation-based evaluation of the actual balance between these sources as measured at the boundary between the port and the city.

2.4. Bivariate polar analysis

To separate the "port" from the "city" components of the AQ variables collected at the port area measurement sites (receptors), data have been analyzed employing the R-package "Openair" bivariate polar analysis (Carslaw et al., 2006; Carslaw and Ropkins, 2012). This processing allows to visualize and quantify how the concentration of a variable (commonly a pollutant) at a receptor point changes as a function of both wind direction and a third parameter (usually wind-speed).

Other approaches employed to identify pollution sources in port areas include source apportionment (SA) analysis, and dispersion modelling. SA has been mainly applied to chemical speciation of PM data to define the type of emitters affecting measured PM loads (Cesari et al., 2014; Pérez et al., 2016; Jeong et al., 2017; Saraga et al., 2019). Whereas source apportionment analysis identifies categories of emitters but not their location, dispersion modelling can identify contributions of various emitters to pollutant loads measured at a receptor site (e.g., Saxe and Larsen, 2004; Gariazzo et al., 2007). However, the detailed temporal and spatial description of emissions and meteorology needed to run these models in an effective way can lead to large discrepancies between modeled and observed data (e.g., Gibson et al., 2013, Casazza et al., 2019). To the end of providing a representative view of the provenance of pollutants in the Civitavecchia port area on the basis of a three-year dataset, the bivariate polar analysis was then preferred to dispersion modelling. This straightforward analysis well suits the Civitavecchia port's conditions since the whole area is flat and maximum distances between main emitters and receptors are of the order of 1–2 km.

Two Openair functions have been chiefly employed to this goal: Polar-Plot and Pollution-Rose. The first one allows to observe bivariate average, weighted mean, and conditional probability function (CPF) distributions of the addressed variable (e.g., Uria-Tellaetxe, and Carslaw, 2014). The second function permits to evaluate the polar-dependent contribution to the mean value of the investigated variables. In particular, the Polar-Plot function permits some discrimination between local and distant sources by exploiting the fact that the first are evidenced at low wind speeds, while the latters are brought to the receptor by increasing wind speeds (e.g., Carslaw et al., 2006). These conditions are expected to hold particularly in a flat area as the Civitavecchia port's one. Combined use of the options available within these two functions allowed us to infer important information about the origin and relevant weight of the addressed pollutants.

3. Data analysis

In Section 3.1 hereafter we analyze first the "long-term" (3-year) record of NO_2, SO_2, and PM_{10} collected at the Arpa Porto station. In Section 3.2, we then address the April 2016 intensive measurements performed by the AEROLAB mobile station at Pier 24.

3.1. The "long-term" picture

3.1.1. Meteorology

Knowledge of local meteorological patterns is important to understand how pollutants are conveyed and dispersed in the area

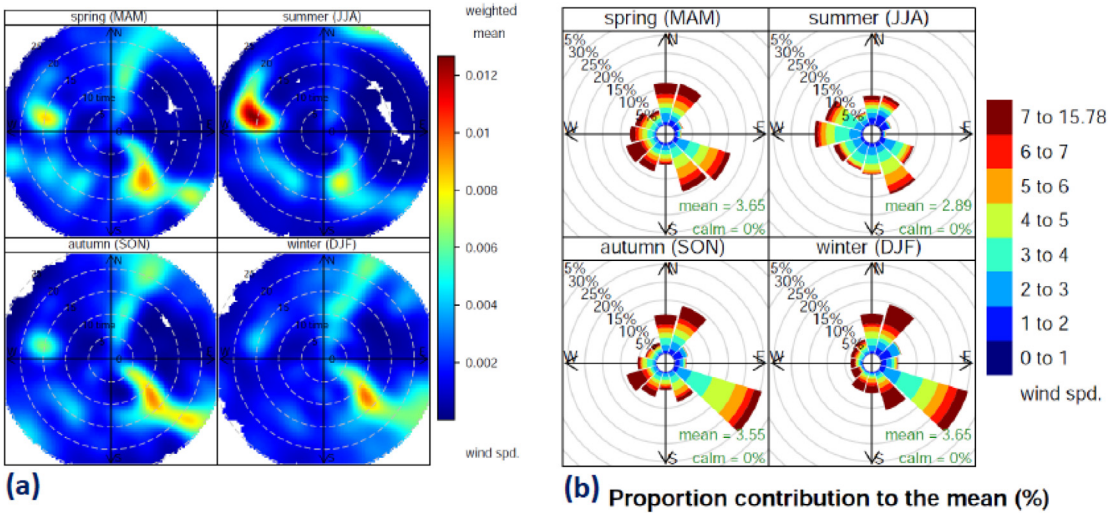

Fig. 2. Typical circulation patterns occurring at the port-city interface station of Arpa Porto in the three-year period 2013–2016: (a) seasonal (spring, summer, autumn, winter) weighted means of the wind speed (color scale) as a function of wind direction (polar), and time of day (radial axis) variables, and (b) seasonal polar distribution of the components of the mean wind speed (m/s). The weighted means in Fig. 2a represent the mean wind speeds weighted by their frequency of occurrence at each wind direction (angle) and time of day (radius, spanning from 0 h UTC at the center to 24 h -UTC at the outer circle).

being studied. Analysis of the Arpa Porto 3-year wind record depicts the typical circulation patterns occurring at the port-city interface. These are summarized in Fig. 2. In particular, Fig. 2a shows the seasonally-resolved weighted mean of the wind speed as a function of wind direction (angle), and time of day (radius, spanning from 0 h UTC at the center to 24 h UTC at the outer circle). This variable represents mean wind speeds weighted by their frequency of occurrence at each wind direction and time of day. Conversely, Fig. 2b illustrates the seasonal polar distribution of the components of the average wind speed. As visible from the maps in Fig. 1, only winds proceeding from the 250° to 340° quadrant can transport air masses from the port to the urban area. Fig. 2b indicates this condition to reach a minimum occurrence (15% of the time) in winter and a maximum (30% of the time) in summer. This is also associated with a sea breeze-type circulation mainly occurring between 10 am and 8 pm (Fig. 2a). Proceeding from angles of 270–300°, these breezes typically convey towards the city the emissions originating at the Ro-Ro passenger and at the cruise-ship piers, that is the port's largest emission sources.

However, Fig. 2 shows the most frequent wind conditions encountered at Arpa Porto to be those proceeding from SE. These occur at all day times over 25% of the time in summer, and 35% of the time in winter (Fig. 2b). This "port pollution-removal" condition is likely associated with the formation of a coastal low-level jet generated by the interaction of S-N pressure gradients and the hills running from the SE to the N-NW, just inland of Civitavecchia (e.g., Stull, 2017). A similar jet pattern (in this case proceeding from N-NE), appears to be generated by the same hills, at their turning towards NE, some 5 km north of the city. These latter conditions occur about 15% of the time in summer, and 25% of the time in the remaining seasons. Both these jet-like patterns decrease in summer, i.e., when pressure gradients minimize.

Overall, these wind statistics indicate that pollutants from the port (and from the Civitavecchia area in general) preferentially disperse to the NW and SW, i.e., away from the city and off the coast. However, diffusion of port's pollution towards Civitavecchia is important in the summer months (about 25% of the time), driven by the sea-breeze pattern, with average wind speeds of 3–4 m/s. Overall, the above-described wind patterns account for about 70–75% of the atmospheric circulation conditions encountered at Civitavecchia during this three-year period, the remaining ones pertaining to diffusion to the N-NE sectors.

3.1.2. "Regulated" pollutants

A long-term representation of the NO_2, SO_2 and PM_{10} pollutants measured at the Arpa Porto station is given in Fig. 3. Based on the addressed three-year dataset, it depicts, respectively: (1) the seasonal mean values of the NO_2, SO_2 and PM_{10} hourly measurements (panels a, b, and c) as a function of wind direction (angle), and time of day (0–24 h UTC, radius), and (2) the polar contribution to the average NO_2, SO_2 and PM_{10} loads (panels d, e, and f). On the basis of the wind-rose shown in Fig. 1d, we assume as originating in the port area all the components reaching the Arpa Porto monitoring station from the angular range 180°–360°. Conversely, the city component reaching the Arpa Porto monitoring station is associated with winds from the 0° to 180° quadrant.

As expected, the NO_2 time-resolved plots (Fig. 3a) show the city-bound contribution to reach a maximum at traffic rush hours (7 am and 7 pm, approximately). This is particularly evident in autumn and winter. Conversely, the port's component spreads over the full 5 am–8 pm time range, peaking at about 4 pm (i.e., when the sea-breeze reaches its maximum, e. g., Fig. 2). The port signal is clearly visible in all the SO_2 records, with a summertime maximum (Fig. 3b). Conversely, the PM_{10} plots do not show dominant fingerprints originating from the port (Fig. 3c). Similarly to what was observed for NO_2, the traffic daily cycle is visible in the city-oriented half-circle in autumn and winter. PM_{10} from the marine quadrants is found to peak mainly before 10 am and at night, not necessarily proceeding from the port hotspots identified by the NO_2 and SO_2 records. As hypothesized by means of the emission estimates discussed in Section 2.3, this point confirms the minor role of port's emissions at determining the PM_{10} load, particularly in winter.

Table 5 reports the Arpa Porto seasonal averages of the three variables addressed here, i.e., NO_2, SO_2 and PM_{10}, as obtained from the analysis of Fig. 3d, 3e and 3f, respectively. Wind speed occurrences obtained from data in Fig. 2b are also included in this table. Components from the 180°–360° quadrant (i.e., originating from the port area and reaching the station), and from the angular range 250°–340° (that is the portion then proceeding from the station towards the city center) are also included in this table as "from

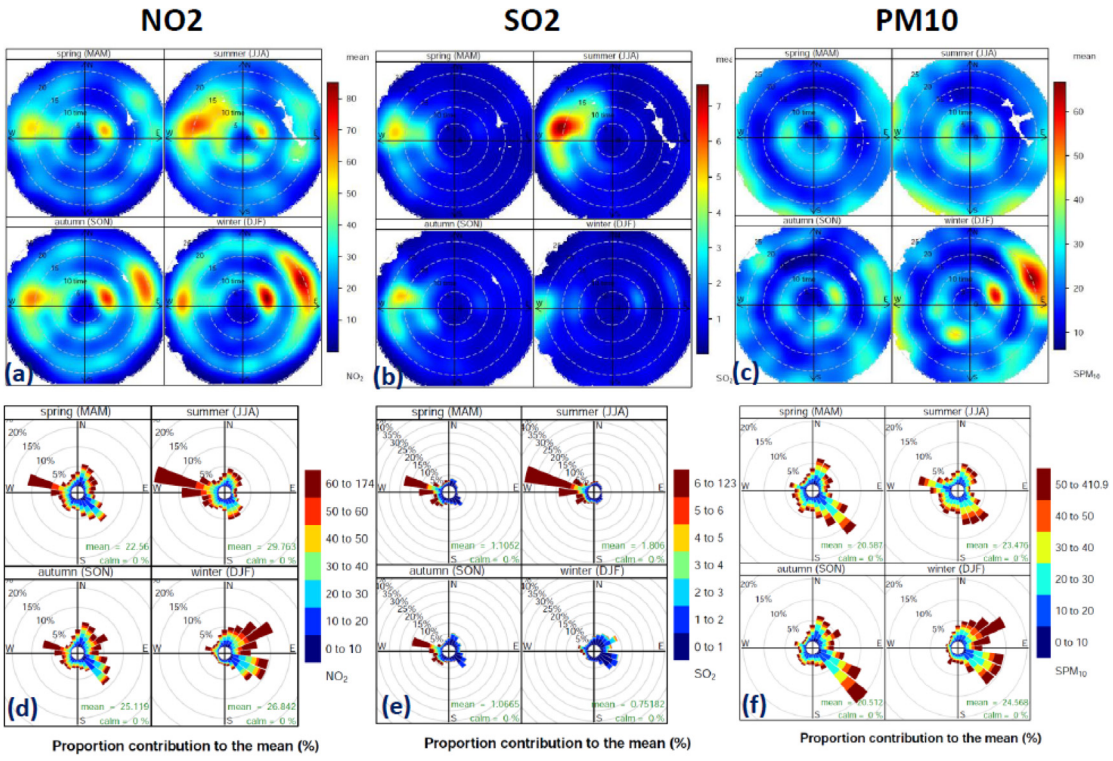

Fig. 3. Seasonal (Spring, Summer, Autumn, Winter) mean values of the NO_2, SO_2 and PM_{10} measurements (panels a, b, and c) as a function of wind direction (polar), and time of day (radial) axes, and polar contribution to the average NO_2, SO_2 and PM_{10} loads (panels d, e, and f), as recorded at the Arpa Porto station during the three-year period 2013–2016.

Table 5
The three-year (2013–2016) statistics of regulated pollutants and wind speeds at the Civitavecchia Arpa Porto station. Wind speed averages "from port" (angular range 180°-360°), and "from port and to the city" (angular range 250°-340°) are given as % occurrences.

Site Arpa Porto	NO_2 [μg/m^3]	SO_2 [μg/m^3]	PM_{10} [μg/m^3]	Wind Speed [m/s]
Year average ± st.dev.	26.3 ± 22.0	1.21 ± 2.7	22.4 ± 18.5	3.4 ± 2.1
Year average from port (% of year average)	11.4 (43%)	0.7 (60%)	7.4 (33%)	40% of wind data from port
Year average from port to Civitavecchia	6.6 (25%)	0.5 (43%)	4.2 (19%)	20% of wind data to Civitavecchia
Winter average	26.8	0.8	24.5	3.7
Winter average from port (% of winter average)	5.4 (20%)	0.2 (30%)	4.9 (20%)	28% of wind data from port, 13% to Civitavecchia
Summer average	29.8	1.8	23.5	2.9
Summer average from port (% of summer average)	16.4 (55%)	1.4 (80%)	11.8 (50%)	50% of wind data from port, 30% to Civitavecchia

port" and "to-the-city" components, respectively. Table 5 shows that in terms of contribution to the mean, 55% of the 29.8 μg/m^3 NO_2 averaged in summer originates from the port area. This reduces to 20% in winter, when the mean NO2 load is of 26.8 μg/m^3. The NO_2 average yearly contribution from the port is of 43%.

In the case of SO_2, 80% of the summer mean value of 1.8 μg/m^3 is contributed by the port area. This reduces to 30% in winter, when the mean SO_2 descends to 0.8 μg/m^3. Highest SO_2 concentrations are generated in the port area, with a yearly average contribution of 60% of the total load. Both SO_2 and NO_2 port components peak at wind directions of 270°–285°, i.e., the direction corresponding to Ro-Ro passenger and cruise ship piers (Fig. 1). In this respect, the intensive observations made at Pier-24 and presented in the following Section 3.2, will help identifying the actual origins of these pollutants.

In terms of contribution to mean PM_{10} values, 50% of the 23.5 μg/m^3 averaged in summer originates from the port area. This reduces to 20% in winter, when the mean PM_{10} rises to 24.5 μg/m^3. In this case, average yearly contribution from the port is of 33%. Both the PM_{10} and NO_2 components from the city show a principal peak at 45°–60°, and a secondary one at 105°–135°, that is, the directions pointing to the closest road traffic source, and to the city center, respectively.

Overall, the analysis of the 3-year record collected at the port-city border indicates that concentrations of regulated pollutants (NO_2, SO_2 and PM_{10}) always kept below EU annual limits, and that the port area (including ship and road movements) represents a minority contribution (33, 43%) to PM_{10} and NO_2, respectively, while contributing 60% of the SO_2 loads. These contributions descend to some 19% for PM_{10}, 25% for NO_2, and 43% for SO_2 if considering the airmasses proceeding to influence the city center. Minimum concentrations were recorded in spring and fall. Summer maxima with respect to winter were observed for SO_2 and NO_2 (attributable to the larger ship traffic and increased sea-breeze condition). A winter maximum of PM_{10} is possibly due to city heating and low-level-jet, south easterly circulation. SO_2 first, and NO_2 act as the clearest tracers of the port's emissions. Finally, neither NO_2 nor SO_2 signals appear to proceed from the power-plants sector (320–330°) towards the city (e. g., Fig. 3).

3.2. Regulated and non-regulated pollutants during the intensive campaign of April 2016

To further investigate the pollution associated with particulate matter in the port area, an intensive observational period was performed in April 2016, in the framework of the CNR's "AirSeaLab" project. The data addressed here were collected by the ISAC-CNR AEROLAB at Pier 24 (high temporal resolution, e.g., Table 1), and by ARPA Lazio at the Arpa Porto station (1-h resolution) in the period 5–26 April 2016. During this intensive campaign, Ro-Ro passenger, cruise, and carrier ships stopped at the Civitavecchia piers 860, 523 and 378 hours, respectively. Median age of these ships was 14, 8 and 9 years. Median mooring times were 5, 12 and 9 hours, respectively. In terms of ship mass-weighed mooring time, this corresponds to approximately 61, 86, and 20 kt*hour per day, respectively. That is, cruise ships embodied the largest mass*permanence-time factor (a proxy for the required amount of energy production) in the port. At the same time, some 56% of the cruise ships calling at the port was running EGCSs (emission gases conditioning systems) for the reduction of both SO_2 and PM emissions.

Polar plots of the regulated pollutants load and contribution to the mean as measured at Arpa Porto during this campaign are presented in Fig. 4, using same plotting formats as in the long-term analysis of Section 3.1.2. Relevant average values and port origins are summarized in Table 6. This shows that measured average loads are all close (well within one standard deviation) to the long-term ones presented in Table 5. During the April 2016 campaign, this station at the port-city boundary registered a harbor contribution to the NO_2, SO_2 and PM_{10} loads of 43%, 73% and 38%, respectively (Table 6 and Fig. 4). As found in the long-term analysis, polar plots of NO_2 and SO_2 presented in Fig. 4 display a clear fingerprint of the port sector. In fact, maxima in NO_2 and SO_2 proceed from 285° (see maps in Fig. 1), with median values of 60 and 6 μg/m^3, respectively (Fig. 4a, b, d, and e). Conversely, a good deal of the PM_{10} originating from the port sector points also to ground mobility corridors (Fig. 4c), that is, it is likely associated with both shipping and road traffic within the port. In analogy with the 3-year statistics, the city emissions originate mainly from the SE, providing important contributions to both PM_{10}, and NO_2 loads (e.g., Fig. 4d and 4f).

Average values of equivalent black carbon (eBC), total particle number concentration (N, sum of particles with diameter 0.008 < D < 10 μm), and total particle volume, V_{10} (that is a proxy for PM_{10}, obtained by summing the volumes of all the particles with D < 10 μm), measured by the AEROLAB at Pier 24 are reported in Table 7. Polar-plots of these variables are presented in Fig. 5. All maximum values in these plots originate from the S-SE area of the port. Only eBC, and to some extent V_{10}, present secondary maxima at low wind speeds, i.e., originating nearby the AEROLAB site. These are possibly generated by local circulation of cargo trains, heavy and light road vehicles reaching nearby piers.

Compared to wintertime measurements performed in the city center of Rome (e.g., Costabile et al., 2017), the average eBC concentration recorded at Pier 24 is about halved (1.3 μg/m^3 vs. 2.6 μg/m^3, while particle number concentrations are almost

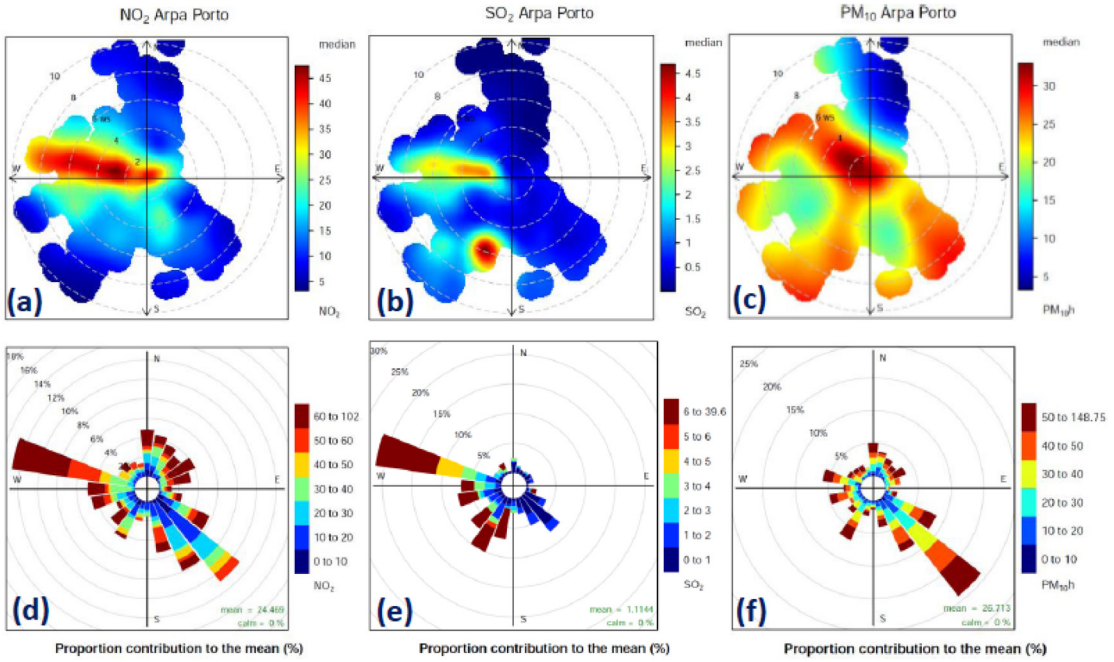

Fig. 4. Median values of the NO_2, SO_2 and PM_{10} loads (panels a, b, and c) as a function of wind direction (polar), and wind speed (radial) axes, and polar contribution to the average NO_2, SO_2 and PM_{10} loads (panels d, e, and f), as recorded at the Arpa Porto station during the April 2016 campaign period.

Table 6
April 2016 campaign: statistics of NO_2, SO_2 and PM_{10} at the Arpa Porto station. Pollutants are defined as arriving from the port area for winds proceeding from the angular range 180°-360°.

	NO_2 [μg/m^3]	SO_2 [μg/m^3]	PM_{10} [μg/m^3]	Wind Speed [m/s]
Campaign average	24.5	1.1	26.7	3.7 (21% to CV)
Average from Port area (% of campaign average)	10.5 (43%)	0.8 (73%)	10.2 (38%)	(40% from port)
Mean value (% contribution) from Ro-Ro passenger piers (285°)	3 (13%)	0.2 (22%)	1.6 (6%)	(7% from 285°)

Table 7
Statistics of equivalent black carbon (eBC), particulate number concentrations (N, size range 0.008 < D < 10 μm), and volume V_{10} (D < 10 μm), as measured by the AEROLAB at Pier 24 during the April 2016 campaign and average contribution from the angular range 150°-185° (Ro-Ro passenger piers).

	eBC [μg/m³]	N [1/cm³]	V_{10} [μcm³/m³]
Campaign average ± st. dev.	1.3 ± 1.6	20,400 ± 22,500	11.7 ± 6.5
Mean from Ro-Ro piers (% contribution to total)	2.0 (45%)	50,000 (58%)	15 (43%)

doubled (20,400 vs. 12,000 cm^{-3}). Some 45%–58% of these average loads originate in the sector 150°–185°, that is, the Ro-Ro passenger piers area (Fig. 1d). In fact, mean loads of 2 μg/m³ for eBC, and 50,000 cm^{-3} for N are observed to originate in this sector (Fig. 5d and e, and Table 7). These loads are rather high with respect to polluted urban sites, particularly in what concerns particle number concentrations. Conversely, even assuming a high aerosol density as of 2 g/cm³, the corresponding V_{10} would translate into an average PM_{10} < 30 μg/m³, that is well below the EU daily limit of 50 μg/m³. Fig. 5 shows that eBC concentrations maximize when proceeding from the Ro-Ro passenger piers segment. The V_{10} plot behaves similarly to eBC, except for some enhancements in the W-SW region, likely originating in the cargo and the cruise-ship sectors. In a similar way, high particle number concentrations (about 90% made of ultrafine particles with D < 100 nm) mainly originate in the port's Ro-Ro passenger area.

The triangulation of sectors originating maximum eBC, and N concentrations at the AEROLAB site (that is the 150°–185° arch), and those originating maximum SO_2 at Arpa Porto (i.e., the 210°–300° arch) places the maximum of particulate emissions in the Ro-Ro passenger zone evidenced in red in Fig. 6. In sea-breeze conditions, this sector is upwind, and less than 1 km apart from the city center.

To better identify properties and origins of pollutants in the addressed port areas, we examined polar-plots of the following variables (Fig. 7): i) the ratio between 40 nm and 100 nm particle number concentrations (dN_{40}/dN_{100}, Fig. 7a), and its reversal, (dN_{100}/dN_{40}, Fig. 7b); ii) the ratio between black carbon concentration (eBC) and particle's volume in the "ultra-fine" size fraction D < 100 nm (V_{100}, Fig. 7c); and iii) the particle's absorption Angstrom exponents (AAE, Fig. 7d), respectively. The dN_{40} vs. dN_{100} relationship provides information about the relevant weight of nucleation-mode particles with respect to accumulation-mode ones. The $eBC/V_{0.1}$ ratio is an indicator of the relative importance of BC within ultra-fine particles. The particle's absorption Angstrom exponent provides information about the relative importance of BC (low AAE) with respect to other light absorbing material as organic carbon or dust (high AAE) in the sampled particles (e.g., Andreae, and Gelencsér, 2006). A further description of these variables will be also given in the following paragraphs.

Examination of Fig. 7 indicates four main combustion sources are likely to drive the average properties of particulate matter in the port:

i) medium/low speed diesel engines running on low-sulfur (still with high contents of HFO) marine diesel oil (MDO), mostly operating in the Ro-Ro passenger and carrier sectors of the port;
ii) medium–high speed diesel engines fitted with EGCS, mainly operating in the cruise-ship and cargo sectors of the port;
iii) diesel, heavy-duty vehicles operating on road; and
iv) light duty vehicles operating either on diesel or gasoline engines.

This interpretation is based on the following arguments:

Ultrafine modes. In plumes emitted by medium/slow speed marine diesels running on MDO, the ratio dN_{40}/dN_{100} (that is between concentrations of "nucleation type" (D ≈ 40 nm) and "accumulation mode" (D ≈ 100 nm particles) is commonly>1 (≫1 for Heavy Fuel Oil). Conversely, this ratio is expected to be < 1 in the case of engines running on MGO (e.g, Anderson et al., 2015) or automotive diesels (e.g., Harris and Maricq, 2001). This is mainly

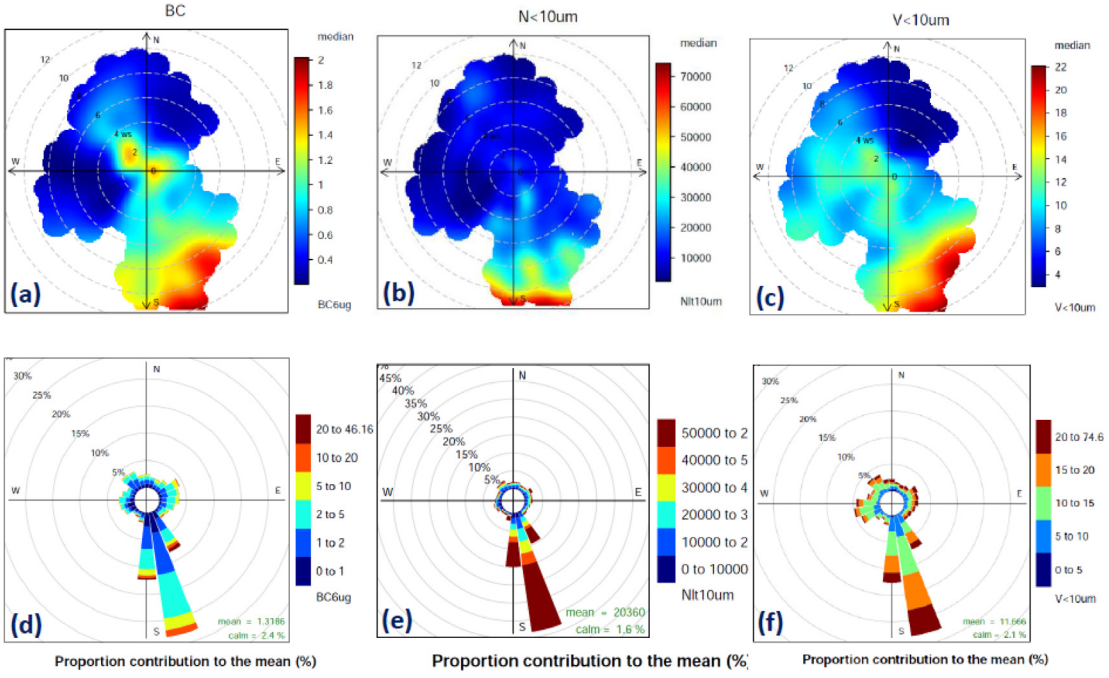

Fig. 5. Median values of the variables eBC, N < 10 μm, and V < 10 μm (panels a, b, and c) as a function of wind direction (polar), and wind speed (radial) axes, and polar contribution to the average eBC, N < 10 μm and V < 10 μm concentrations (panels d, e, and f), as recorded at the AEROLAB during the April 2016 campaign at Pier 24.

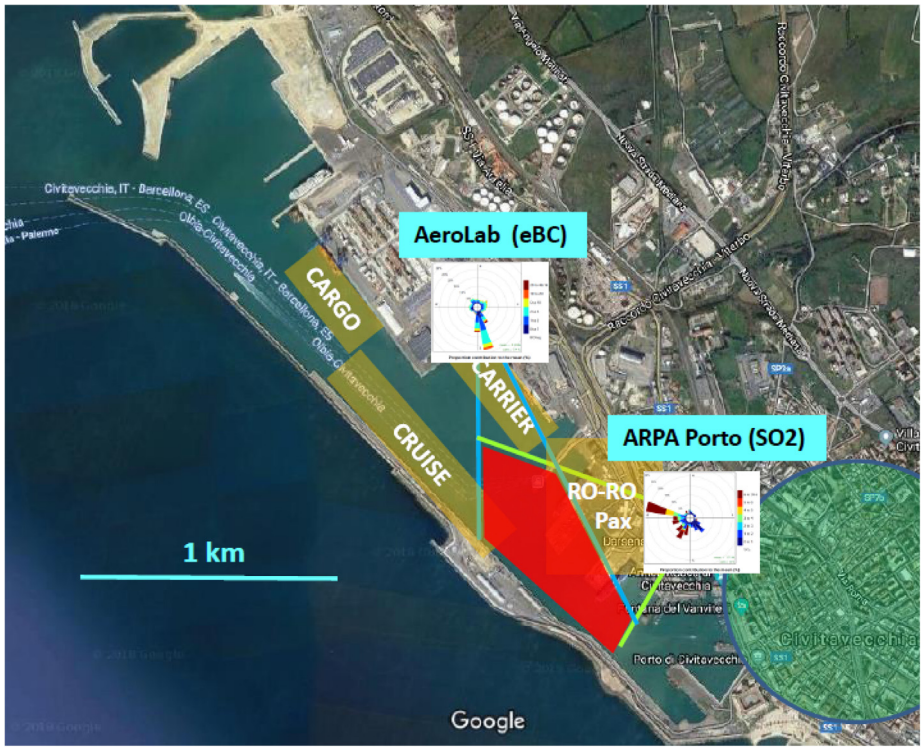

Fig. 6. Triangulation between origins of maximum eBC sources (as measured by the AEROLAB at Pier 24), and maximum SO_2 sources (as measured at Arpa Porto), during the April 2016 campaign. The Civitavecchia city center is indicated by the blue circle at the bottom right end of the figure. (For interpretation of the references to color in this figure legend, the reader is referred to the web version of this article.)

due to the high concentration of residuals (heavy metals, ash and sulfur) present in marine unrefined oils (as MDO), a condition leading to an enhanced generation of "nucleation mode" nanoparticles (e.g., Kasper et al., 2007; Anderson et al., 2015; Streibel, 2016; ICCT, 2016), and black carbon (Lack and Corbett, 2012). In addition to the use of HFO and MDO, presence of "nucleation mode" particles in marine emissions is also associated with low engine load operations (e.g., ICCT, 2016). As opposite, and similarly to road diesels, marine diesel engines running at optimal loads tend to emit particles centered at about 100 nm (Harris and Maricq, 2001). Recent cruise ships often run on battery-fed electric motors, whose energy is generated by diesel engines operating at optimal speed. Emissions from engines using less-refined oils should then present high dN_{40}/dN_{100} ratios. In this respect, the SMPS-derived dN_{40}/dN_{100} ratios presented in Fig. 7a maximize in the Ro-Ro passengers sector first, with secondary maxima in the carriers (South) sector. Conversely, the inverse ratio dN_{100}/dN_{40} (Fig. 7b) presents maxima in the cruise ship sector (SW and W of Pier 24), and in the road traffic areas of the port (NW to SW half circle), particularly in low-wind conditions, i.e., for advected air associated with nearby yards, where cars and containers were handled before shipping.

Specific eBC content. Even though most of the eBC emissions originate from the Ro-Ro passengers sector (Fig. 5d), black carbon contents at specific particles volume (the eBC/ V_{100} ratio of Fig. 7c) are highest along the road traffic areas of the port. These areas are characterized by heavy-duty vehicle operations in the NW (port construction, cargo loading, and vehicle maneuvering areas) and eastern (heavy duty vehicles and trains) sectors, and by light vehicle traffic in the SE, and NE sectors. In fact, Kasper et al. (2007) points out that the ratio between particle number and BC concentrations is higher in low-speed marine diesels with respect to light vehicle diesels. Interestingly enough, cruise ships are found to emit less BC (Fig. 5a) and less BC per aerosol unit volume than all other ships and ground vehicles operating in the port (Fig. 7c). In the comparison of ship emissions, this is possibly attributable to cruise ships employing: i) a better fuel quality (as inferred by the previous point); ii) EGCS devices on 56% of the calling vessels; iii) engines operating at optimal regimes (e.g., ICCT, 2016). In the ship vs. road-vehicle comparison, the unbalance possibly depends on to the higher BC emission factors characterizing road vehicles with respect to ship engines (e. g., Ježek et al., 2015, Zavala et al., 2017; ICCT, 2016). In fact, the ICCT, 2016 tests report distillate fuels (MGO) to generate the lowest BC emissions, followed by conventional HFO. The highest BC emission factors were found to be associated with the low sulfur, residual fuel (MDO) tested.

Light absorption coefficients. The absorption Angstrom exponent (AAE) is a measure of the spectral variation of the aerosol absorption coefficient. Amongst light absorbing aerosols, black carbon is characterized by low spectral variation of the absorption coefficient, i.e., $AAE \leq 1$. Conversely, light absorption of organic aerosols and mineral dust shows a marked spectral dependence ($AAE > 1$), e.g., Andreae, and Gelencsér, 2006, Bond et al., 2013. Analysis of the AAE plot in Fig. 7d indicates that both cruise ships (W-SW sector), and light-vehicle road traffic (NE sector) are mainly characterized by organic carbon type emissions ($AAE > 1$). Such finding can be explained by the higher proportion of organics gasoline cars emit with respect to both diesel cars (a factor of about 10 higher) and ship diesels (about two-times higher), e.g., EEA (2016). Conversely, prevailing BC conditions ($AAE \leq 1$) are confirmed to dominate aerosol properties in the whole Ro-Ro passenger berthing areas, in the port channel leading to the open sea (associated to medium wind speeds), and in the new port construction sectors to the NW.

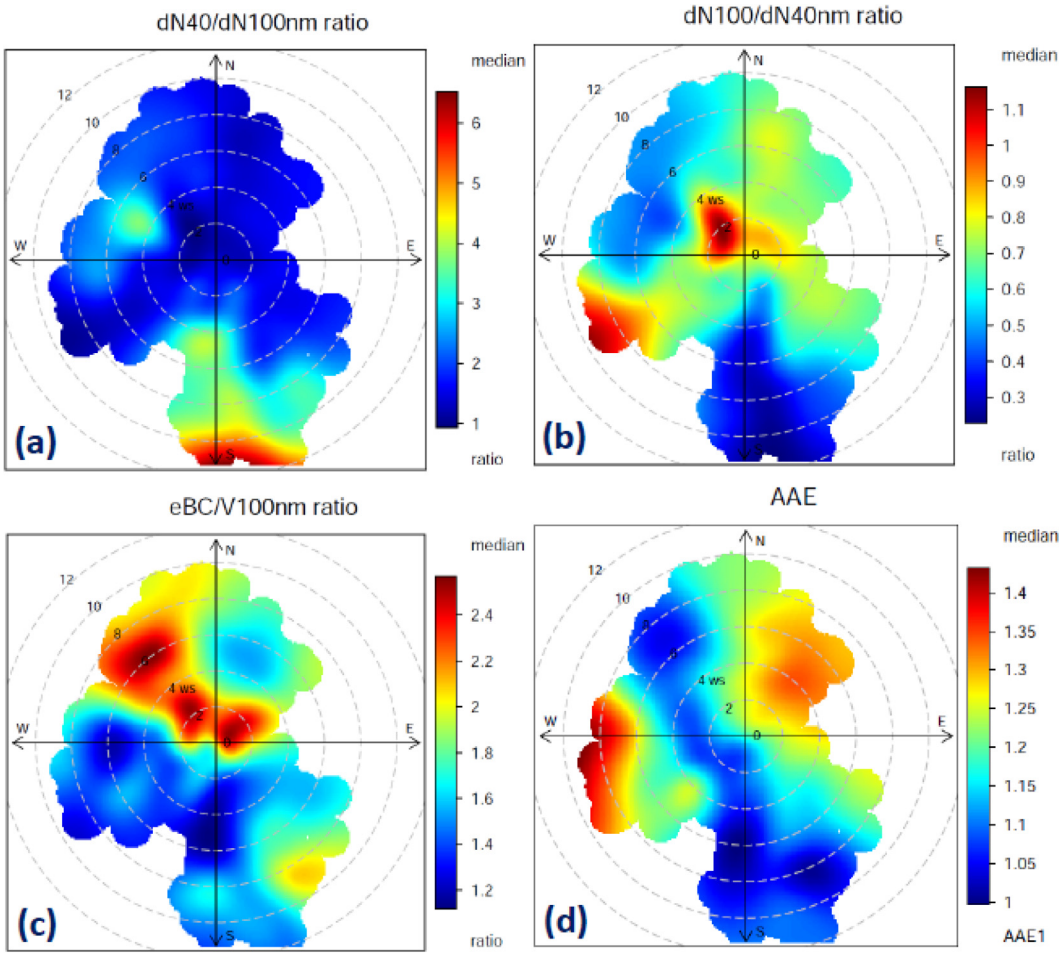

Fig. 7. Ratio of particle number size distribution's channels at 40 and 100 nm: a) (dN40/dN100, and b) dN100/dN40. c) ratio between black carbon concentration (eBC) and particle's volume in the size fraction D < 100 nm ($V_{0.1}$). d) particle's absorption Angstrom exponents (AAE). Plots' plane variables are wind speed (radial) and direction (angle).

4. Discussion

Principal goal of this paper was the separation of emissions originated in the port area from the ones pertaining to the city of Civitavecchia. This was achieved by the bivariate data analysis of AQ measurements collected over three years at the exact border between the city and the port, that is, a city area where the impact of port emissions is expected to be the highest. This analysis identified main points of emission and their contribution to the measured loads of regulated pollutants as NO_2, PM_{10}, and SO_2. The overall contribution from the port area vs. the one originating from the city area could then be evaluated for these three markers. Combination of intensive observations from two receptor stations made in April 2016, also allowed to infer piers and ship categories emitting the highest amounts of UFP, eBC, NO_2, PM_{10}, and SO_2. Main strength of this analysis resides in its direct, statistical representation of real data (e.g., Carslaw and Beevers, 2013). Main limitations of the approach are related to the attribution of pollutant sources based essentially on provenance and speed of winds during measurements. In this respect, both the flatness of the investigated area and the short distances (ranging between 50 and 2000 m) separating emitters from observing stations support the reliability of the results presented in the paper. Considering the type of data employed (a 3-year record of hourly NO_2, PM_{10}, and SO_2) and a 1-month record of aerosol size distributions and eBC concentrations at minute time resolution, analogous results could only be obtained by high resolution dispersion modeling (e.g., Gibson et al., 2013). In addition to the general port vs. city pollutants share obtained in our analysis, dispersion modeling might also isolate contributions of single emitters. At the same time, such an approach would have required a huge effort to define time evolution and properties of the emissions, and high resolution meteorological dispersion parameters along a 3-year timeframe. This could possibly lead to important errors in the case of rapidly varying pollutants as eBC, PM_{10}, and particle number concentration (e.g., Gibson et al., 2013). We therefore believe the results provided in this paper represent a reasonable estimate of the whole port's area contribution to air pollution at the port-city border and a good quantification of sources of unregulated, still important pollutants as UFP and BC.

5. Conclusions

In spite of air pollution records well below the limits established by the EU Air Quality Directive (2008/50), the city of Civitavecchia suffers from some health issues with respect to the regional average. Main emissions in this area are generated by two collocated power stations emitting out of high stacks some 4 km north of the city, by the port, and by the city's road traffic and heating. These four sources (considering the two power stations as one) were estimated to contribute some 5500, 1000, 300, and 100 t/y NO_2; 60, 40, 20, and 100 t/y PM_{10}, and 2000, 30, 0, and 10 t/y SO_2, respectively. In this context, measurements of

atmospheric pollutants in the Civitavecchia port area have been studied in relation to wind parameters both on a long-term (3-year monitoring) and on a short-term (one-month intensive observations) basis. The study employed a bivariate polar analysis of "receptor type" observations performed at fixed monitoring stations operated at the port-city boundary, and within the port itself.

Analysis of the 3-year dataset indicated that pollutants from the port (and from the Civitavecchia area in general) preferentially diffuse to the NW and SW directions, i.e., away from the city. This happens thanks to the frequent formation of low-level jets by the nearby hills. Diffusion of port's pollution to the city of Civitavecchia maximizes in spring and summer, mainly between 10 and 20 UTC, following a sea-breeze pattern with average wind speeds of 3–4 m/s. The long-term measurements collected at the port-city boundary (Arpa Porto station) confirmed that concentrations of regulated pollutants (NO_2, SO_2 and PM_{10}) always kept below EU limits. The port area (including ship and ground operations) contributed respectively 33% (7.4 $\mu g/m^3$), 43% (11.4 $\mu g/m^3$), and 60% (0.7 $\mu g/m^3$) of the PM_{10}, NO_2, and SO_2 loads observed at Arpa Porto. Some 4.2 $\mu g/m^3$ PM_{10}, 6.6 $\mu g/m^3$ NO_2, and 0.5 $\mu g/m^3$ SO_2 were estimated to then proceed to influence the city center annual loads. Out of these three species, SO_2 first and NO_2 were found to be the clearest tracers of the port emissions. In particular, SO_2 best correlates with port origins and with the seasonal variation of the port's marine traffic. Neither the NO_2 nor the SO_2 records evidenced clear footprints from the two power plants.

Specifically addressing BC contents, ultrafine particles concentration and size distribution, the intensive campaign carried-out within the port, in April 2016, allowed to unveil some important features of the particulate matter origins and properties in the port area. In this spring period, cruise ships first, and Ro-Ro passenger ships represented the largest hotelling masses, i.e., energy production in the port. Some 56% of the cruise ships calling at the port was employing emission gases conditioning systems to reduce both SO_2 and PM emissions. During this campaign, the Arpa Porto station registered a harbor contribution to the PM_{10}, NO_2, and SO_2 loads of 38%, 43%, and 73%, respectively. These values are in good agreement with the 3-year averages observed at the same station. As found by the long-term analysis. NO_2 and SO_2 represented the clearest fingerprint of the port sector. Both these components originated mainly from the Ro-Ro passenger and cruise ship piers.

Measurements of equivalent black carbon (eBC), size resolved particle number concentration, and particle volume (V_{10}) collected at Pier 24 by our mobile AEROLAB, indicated maximum number concentrations to originate in the S-SE area of the port. Black carbon, and to some extent V_{10}, presented secondary maxima from sources nearby the AEROLAB site (located at the port's center). These are possibly due to local traffic of cargo trains, heavy and light-duty vehicles reaching nearby piers. Particle's number concentrations were dominated by emissions from the Ro-Ro ferry sectors. The average eBC load recorded at Pier 24 was about half the one measured in downtown Rome, in winter (1.3 $\mu g/m^3$ vs. 2.6 $\mu g/m^3$). Conversely, particle number concentrations were almost twice as high (20,400 cm^{-3} vs. 12,000 cm^{-3}). Some 45%–58% of these average loads originated from the sector 135°–185°. Triangulation with SO_2 maxima observed at Arpa Porto indicates this to coincide with the Ro-Ro passenger piers area. Monthly median loads of 2 $\mu g/m^3$ for eBC, and 50,000 cm^{-3} for N were observed to proceed from this "hot spot" to Pier 24, while PM_{10} did not exceed 30 $\mu g/m^3$.

The combined analysis of particle's size distributions and eBC allowed allocating some different engine and fuel sources. In particular, four main combustion sources were suggested to determine the average properties of particulate matter emitted in the port: i) medium/low speed diesel engines operating on low-sulfur (still with high contents of HFO elements) marine diesel oil, mostly operating in the Ro-Ro passenger and carriers sectors of the port; ii) medium–high speed diesel engines fitted with EGCS, mainly operating in the cruise ship and cargo sectors of the port; iii) diesel, heavy-duty vehicles operating on road and/or rail; and iv) light duty vehicles operating either on diesel or gasoline engines.

Cruise ships were observed to emit less BC, and less BC per aerosol unit volume than all other ships and ground vehicles operating in the port. In the case of ship emissions, this is possibly attributable to cruise ships employing: i) better fuel quality; ii) EGCS devices; iii) engines operating at optimal regimes, or to a combination of these factors. In the ship vs. road-vehicle comparison, the differences could depend on the higher BC emission factors characterizing road vehicles with respect to ship engines.

All these evidences substantiate the picture of the Civitavecchia port-city boundary (that is, the city area most affected by the port's activities) as standing below EU limits in terms of regulated pollutants (NO_x, SO_2, and PM_{10}). The port itself is estimated to contribute some 33% and 43% of the PM_{10} and NO_2 loads at Arpa Porto, with diminishing impact at the city center. Chief origins of port's NO_2 coincide with Ro-Ro passenger and cruise ship sectors. When focusing on currently unregulated pollutants, the port is shown to contribute very high concentrations of ultra-fine particles and high concentrations of black carbon, manly generated in the Ro-Ro passenger and carrier sectors. During sea-breeze conditions (more frequent in summer, when ship traffic is at its maximum) this "hot spot" sits upwind and less than 1 km apart from the city center. An impact onto the city air quality is therefore expected out of these unregulated emissions. This could be mitigated by moving north the relevant piers, and/or by reducing/improving the quality of the emissions. To reduce citizen's exposure to these pollutants, specific alerts could be issued when meteorological conditions favor the diffusion of port emissions to the city.

Acknowledgments

We wish to thank the Rome Ports Authority for providing data and information about the Civitavecchia ship traffic. We thank ARPA Lazio for sharing the Civitavecchia air quality data employed in this paper. The April 2016 intensive field campaign was run in the framework of the "Air-Sea-Lab", CNR Twin Laboratory Project, 2015, and with the logistical support of the Rome Ports Authority.

References

Aksoyoglu, S., Baltensperger, U., Prévôt, A.S.H., 2016. Contribution of ship emissions to the concentration and deposition of air pollutants in Europe. Atmos. Chem. Phys. 16, 1895–1906. https://doi.org/10.5194/acp-16-1895-2016.

Anderson, M., Salo, K., Hallquist, Å.M., Fridell, E., 2015. Characterization of particles from a marine engine operating at low loads. Atmos. Env. 101, 65–71. https://doi.org/10.1016/j.atmosenv.2014.11.009.

Andreae, M.O., Gelencsér, A., 2006. Black carbon or brown carbon? The nature of light-absorbing carbonaceous aerosols. Atmos. Chem. Phys. 6, 3131–3148. https://doi.org/10.5194/acp-6-3131-2006.

Barregård, L., Fridell, E., Winnes, H., 2014. Particle emissions from ships, targeting the environmental sustainability of European shipping: the need for innovation in policy and technology. EPSD Report 6, 20–30.

Bauleo, L., Bucci, S., Antonucci, C., Sozzi, R., Davoli, M., Forastiere, F., Ancona, C., 2018. Long-term exposure to air pollutants from multiple sources and mortality in an industrial area: a cohort study. Occup. Environ. Med. Published Online First 14, 2018. https://doi.org/10.1136/oemed-2018-105059.

Benbrahim-Tallaa, L., Baan, R.A., Grosse, Y., Lauby-Secretan, B., El Ghissassi, F., Bouvard, V., Guha, N., Loomis, D., Straif, K., 2012. Carcinogenicity of diesel-engine and gasoline-engine exhausts and some nitroarenes. Lancet 13 (7), 663–664.

Bond, T.C., Doherty, S.J., Fahey, D.W., Forster, P.M., Berntsen, T., De Angelo, B.J., 2013. Bounding the role of black carbon in the climate system: A scientific assessment Retrieved from J. Geophys. Res. Atmospheres 118 (11), 5380–5552. https://doi.org/10.1002/jgrd.50171.

Buhaug, Ø., Corbett, J.J., Endresen, Ø., Eyring, V., Faber, J., Hanayama, S., Lee, D.S., Lee, D., Lindstad, H., Markowska, A.Z., Mjelde, A., Nelissen, D., Nilsen, J., Pålsson, C., Winebrake, J.J., Wu, W., Yoshida, K., 2009. (2009), Second IMO GHG study 2009. Prevention of air pollution from ships, International Maritime Organization (IMO), London.

Carslaw, D.C., Beevers, S.D., Ropkins, K., Bell, M.C., 2006. Detecting and quantifying aircraft and other on-airport contributions to ambient nitrogen oxides in the vicinity of a large international airport". Atmos. Environ. 40 (28), 5424–5434.

Carslaw, D.C., Ropkins, K., 2012. Openair - an R package for air quality data analysis. Environ. Modell. Software. 27–28, pp. 52–61.

Carslaw, D.C., Beevers, S.D., 2013. Characterising and understanding emission sources using bivariate polar plots and k-means clustering. Environ. Modell. Software 40, 325–329. https://doi.org/10.1016/j.envsoft.2012.09.005.

Corbett, J.J., Winebrake, J.J., Green, E.H., Kasibhatla, P., Eyring, V., Lauer, A., 2007. Mortality from ship emissions: A global assessment. Environ. Sci. Technol. 41 (24), 8512–8518. https://doi.org/10.1021/es071686z.

Casazza, M., Lega, M., Jannelli, E., Minutillo, M., Jaffe, D., Severino, V., Ulgiatic, S., 2019. 3D monitoring and modelling of air quality for sustainable urban port planning: Review and perspectives. J. Cleaner Prod. 231, 1342–1352. https://doi.org/10.1016/j.jclepro.2019.05.257.

Cesari, D., Genga, A., Ielpo, P., Siciliano, M., Mascolo, G., Grasso, F.M., Contini, D., 2014. Source apportionment of PM2.5 in the harbor-industrial area of Brindisi (Italy): Identification and estimation of the contribution of in-port ship emissions. Sci. Total Environ. https://doi.org/10.1016/j.scitotenv.2014.08.007.

Costabile, F., Alas, F.H., Aufderheide, M., Avino, P., Amato, F., Barnaba, F., Berico, M., Bernardoni, V., Calzolai, G., Canepari, S., Casasanta, G., Ciampichetti, S., Cordelli, E., Di Ianni, A., Di Liberto, L., Facchini, M.C., Frasca, D., Gilardoni, S., Grollino, M. G., Gualtieri, M., Lucarelli, F., Malaguti, A., Manigrasso, M., Montagnoli, M., Nava, S., Padoan, E., Perrino, C., Petralia, E., Petenko, I., Simonetti, G., Tranfo, G., Valli, G., Valentini, S., Vecchi, R., Volpi, F., Gobbi, G.P., 2017. First Results of the "Carbonaceous Aerosol in Rome and Environs (CARE)" Experiment: Beyond Current Standards for PM10. Atmosphere 8 (249). https://doi.org/10.3390/atmos8120249.

Cullinane, K., 2014. Introduction and overview to: Targeting the environmental sustainability of european shipping: The need for innovation in policy and technology. EPSD Report 6, 5–16.

Deniz, C., Kilic, A., Civkaroglu, G., 2010. (2010) Estimation of shipping emissions in Candarli Gulf, Turkey. Environ. Monitor. Assess 271, 219–228.

EEA, 2013, European Environment Agency, The impact of international shipping on European air quality and climate forcing, Technical report No 4, 2013.

EEA, 2016, EMEP/EEA air pollutant emission inventory guidebook 2016 Technical guidance to prepare national emission inventories, Report No 21/2016, ISSN 1977-8449, 2016.

EEA, 2017a, Aviation and shipping - impacts on Europe's environment: Transport and Environment Reporting Mechanism (TERM) report, EEA Report No 22/2017a.

EEA, 2017b, 'Emissions of air pollutants from transport', TERM indicator 003, European Environment Agency (https://www.eea.europa.eu/data-and-maps/indicators/transport-emissions-of-air-pollutants-8/transport-emissions-of-air-pollutants-4), 2017b.

EEA, 2017c, Final energy consumption by mode of transport, Indicator Assessment, Prod-ID: IND-113-en, Also known as: TERM 001, https://www.eea.europa.eu/downloads/a51b7b0b6e8a4873a8f1e6b85154dd17/1512485328/assessment-8.pdf, 2017c.

EIA, U.S. Energy Information Administration, International Energy Outlook, DOE/EIA-0484 (2016), https://www.eia.gov/outlooks/ieo/pdf/0484(2016).pdf, 2016.

ENEL, 2016, Dichiarazione ambientale, Impianto termoelettrico Torrevaldaliga Nord Civitavecchia, 2012.

Eyring, V., Isaksen S.A., I., Berntsen, T., Collins J., W., Corbett J., J., Endresen, O., Grainger G., R., Moldanova, J., Schlager, H., Stevenson S., D., 2010. Transport impacts on atmosphere and climate: Shipping. Atmospheric Environment 44, 4735–4771. https://doi.org/10.1016/j.atmosenv.2009.04.059.

Eyring, V., Köhler, H.W., van Aardenne, J., Lauer, A., 2005. Emissions from international shipping. J. Geophys Res. 110, D17305.

Fano, V., Michelozzi, P., Ancona, C., Capon, A., Forastiere, F., Perucci, C.A., 2004. Occupational and environmental exposures and lung cancer in an industrialized area in Italy. Occup. Envir. Med. 61, 757–763.

Fano, V., Forastiere, F., Papini, P., Tancioni, V., Di Napoli, A., Perucci, C.A., 2006. Mortalità e ricoveri ospedalieri nell'area industriale di Civitavecchia, anni 1997–2004. Epidemiologia e Prevenzione 30, 221.226.

Gariazzo, C., Papaleo, V., Pelliccioni, A., Calori, G., Radice, P., Tinarelli, G., 2007. Application of a Lagrangian particle model to assess the impact of harbour, industrial and urban activities on air quality in the Taranto area, Italy. Atmos. Environ. 41 (30), 6432–6444. https://doi.org/10.1016/j.atmosenv.2007.06.005.

Gibson, M.D., Kundu, S., Satish, M., 2013. Dispersion model evaluation of PM2.5, NOx and SO2 from point and major line sources in Nova Scotia, Canada using AERMOD Gaussian plume air dispersion model. Atmos. Pollut. Res. 4 (2), 157–167. https://doi.org/10.5094/APR.2013.016.

Harris, Stephen J., Maricq, M.Matti, 2001. Signature size distributions for diesel and gasoline engine exhaust particulate matter. J. Aerosol. Sci. 32 (6), 749–764. https://doi.org/10.1016/S0021-8502(00)00111-7.

ISPRA, 2009, La disaggregazione a livello provinciale dell'inventario nazionale delle emissioni, Report 92, ISBN 978-88-448-0392-6, 2009.

ISPRA, 2010, Trasporto su strada, Inventario nazionale delle emissioni e disaggregazione provinciale, Report #124, ISBN 978-88-448-0466-4, 2010.

ISPRA, 2014, Linee guida per le attività di assicurazione/controllo qualità (QA/QC) per le reti di monitoraggio per la qualità dell'aria ambiente, ai sensi del D.Lgs. 155/2010 come modificato dal D.Lgs. 250/2012, Report #108, ISBN: 978-88-448-0647-7, 2014.

ISPRA, 2018, Italian Emission Inventory 1990-2016, Informative Inventory Report 284, ISBN 978-88-448-0891-4, 2018.

ICCT, 2016. Black Carbon Measurement Methods and Emission Factors from Ships. International Council on Clean Transportation, Washington D.C., USA, pp. 1–182.

Jeong, Ju-Hee, Shon, Zang-Ho, Kang, Minsung, Song, Sang-Keun, Kim, Yoo-Keun, Park, Jinsoo, Kim, Hyunjae, 2017. Comparison of source apportionment of PM 2.5 using receptor models in the main hub port city of East Asia: Busan. Atmos. Environ. 148, 115–127. https://doi.org/10.1016/j.atmosenv.2016.10.055.

Ježek, I., Katrašnik, T., Westerdahl, D., Močnik, G., 2015. Black carbon, particle number concentration and nitrogen oxide emission factors of random in-use vehicles measured with the on-road chasing method. Atmos. Chem. Phys. 15, 11011–11026. https://doi.org/10.5194/acp-15-11011-2015.

Kasper, A., Aufdenblatten, S., Forss, A., Mohr, M., Burtscher, H., 2007. Particulate emissions from a low-speed marine diesel engine. Aerosol Sci. Technol. 41 (1), 24–32. https://doi.org/10.1080/02786820601055392).

Lack, D.A., Corbett, J.J., 2012. Black carbon from ships: a review of the effects of ship speed, fuel quality and exhaust gas scrubbing. Atmos. Chem. Phys. 12 (9), 3985–4000.

Maragkogianni, A., Papaefthimiou, S., Zopounidis, C., 2016. Mitigating shipping emissions in European ports. Springer Briefs Appl. Sci. Technol. https://doi.org/10.1007/978-3-319-40150-8_1.

Moldanova, J., Fridell, E., Winness, H., Holmin-Fridell, S., Boman, J., Jedynska, A., Tishkova, V., Demirdjian, B., Joulie, S., Bladt, H., Ivleva P., N., Niessner, R., 2013. Physical and chemical characterisation of PM emissions from two ships operating in European Emission Control Areas. Atmos. Meas. Tech. 6, 3577–3596. https://doi.org/10.5194/amt-6-3577-2013.

Murena, F., Mocerino, L., Quaranta, F., Toscano, D., 2018. Impact on air quality of cruise ship emissions in Naples, Italy. Atmos. Environ. 187, 70–83. https://doi.org/10.1016/j.atmosenv.2018.05.056.

Oeder, S., Kanashova, T., Sippula, O., Sapcariu, S.C., Streibel, T., Arteaga-Salas, J.M., 2015. Particulate matter from both heavy fuel oil and diesel fuel shipping emissions show strong biological effects on human lung cells at realistic and comparable in vitro exposure conditions. PLoS ONE 10, (6). https://doi.org/10.1371/journal.pone.0126536 e0126536.

Pérez, Noemí, Pey, Jorge, Reche, Cristina, Cortés, Joaquim, Alastuey, Andrés, Querol, Xavier, 2016. Impact of harbour emissions on ambient PM 10 and PM 2.5 in Barcelona (Spain): Evidences of secondary aerosol formation within the urban area. Sci. Total Environ. 571, 237–250. https://doi.org/10.1016/j.scitotenv.2016.07.025.

Petzold, A., Weingarner, E., Hasselbach, J., Lauer, P., Kurok, C., Fleisher, F., 2010. Physical Properties, Chemical Composition, and Cloud Forming Potential of Particulate Emissions from a Marine Diesel Engine at Various Load Conditions. Environmental Science and Technology 44 (10), 3800–3805. https://doi.org/10.1021/es903681z.

Psaraftis, H.N., Kontovas, C.A., 2009. CO_2 emission statistics for the world commercial fleet. WMU, J. Maritime Affairs 8, 1–25.

Saraga, D.E., Tolis, E.I., Maggos, T., Vasilakos, C., Bartzis, J.G., 2019. PM2.5 source apportionment for the port city of Thessaloniki, Greece. Sci. Total Environ. 650 (2), 2337–2354. https://doi.org/10.1016/j.scitotenv.2018.09.25010.

Saxe, H., Larsen, T., 2004. Air pollution from ships in three Danish ports, August 2004. Atmos. Environ. 38 (24), 4057–4067. https://doi.org/10.1016/j.atmosenv.2004.03.055.

Sofiev, Mikhail, Winebrake, James J., Johansson, Lasse, Carr, Edward W., Prank, Marje, Soares, Joana, Vira, Julius, Kouznetsov, Rostislav, Jalkanen, Jukka-Pekka, Corbett, James J., 2018. Cleaner fuels for ships provide public health benefits with climate tradeoffs. Nat Commun 9 (1). https://doi.org/10.1038/s41467-017-02774-9.

Stull, R., Practical Meteorology: An Algebra-based Survey of Atmospheric Science, Univ. of British Columbia, 940 pages, ISBN 978-0-88865-283-6, 2017.

Streibel, T. et al., 2016. Aerosol emissions of a ship diesel engine operated with diesel fuel or heavy fuel oil. RECENTADVANCES IN CHEMISTRYAND THE ENVIRONMENT. Springer. https://doi.org/10.1007/s11356-016-6724-z.

Thunis, P., Degraeuwe, B., Pisoni, E., Trombetti, M., Peduzzi, E., Belis, C.A., Wilson, J., Clappier, A., Vignati, E., 2018. PM2.5 source allocation in European cities: A SHERPA modelling study. Atmos. Env. 187 (9), 3–106. https://doi.org/10.1016/j.atmosenv.2018.05.062.

Tzannatos, E., 2010. Ship emissions and their externalities for the port of Piraeus - Greece. Atmospheric Environment, 44, 400-407, doi:10.1016/j.atmosenv.2009.10.024, 2010.

UNCTAD, 2017, United Nations Conference on Trade and Development, Review of Maritime transport, ISBN 978-92-1-112922-9, UNCTAD/RMT/2017, 2017.

UNCTAD, 2012. United Nations Conference on Trade and Development, Review of Maritime Transport 2012, UNCTAD/RMT/2012.. United Nations. ISBN 978-92-1-112860-4.

Uria-Tellaetxe, I., Carslaw, D.C., 2014. Conditional bivariate probability function for source identification". Environ. Modell. Software 59, 1–9. https://doi.org/10.1016/j.envsoft.2014.05.002.

Viana, M., Hammingh, P., Colette, A., Querol, X., Degraeuwe, B., de Vlieger, I., van Aardenne, J., 2014. Impact of maritime transport emissions on coastal air quality in Europe. Atmos. Environ. 90, 96–105.

Whall, C., Cooper, D., Archer, K., Twigger, L., Thurston, N., Ockwell, D., McIntyre, A., Ritchie, A., 2002. Quantification of Emissions from Ships Associated with Ship Movements between Ports in the European Community. Final Report 0617702121. Entec, UK Limited, Norwich, UK, 2002.

WHO, Health effects of black carbon, WHO Regional Office for Europe, ISBN: 978 92 890 0265 3, 2012.

WHO, Health risks of air pollution in Europe – HRAPIE project, Recommendations for concentration–response functions for cost–benefit analysis of particulate matter, ozone and nitrogen dioxide, 2013.

Winebrake J., J., Corbett J., J., Green H., E., Lauer, A., Eyring, V., 2009. Mitigating the Health Impacts of Pollution from Oceangoing Shipping: An Assessment of Low-Sulfur Fuel Mandates. Environmental Science and Technology 43 (13), 4776–4782. https://doi.org/10.1021/es803224q.

Winnes, H., Fridell, E., 2009. Particle emissions from ships: dependence on fuel type. J. Air Waste Manag. Assoc. 59 (12), 1391–1398. https://doi.org/10.3155/1047-3289.59.12.1391.

WMO/GAW, Aerosol Measurement Procedures, Guidelines and Recommendations, GAW Report 227, 2016.

Zavala, M., Molina T., L., Yacovitch I., T., Fortner C., E., Roscioli R., J., Floerchinger, C., Herndon C., S., Kolb E., C., Knighton B., W., Paramo, V.H., Zirath, S., Mejia, J.A., Jazcilevich, A., 2017. Emission factors of black carbon and co-pollutants from diesel vehicles in Mexico City. Atmos. Chem. Phys., 17, 15293–15305. https://doi.org/10.5194/acp-17-15293-2017.